



Bacterial adhesion inhibition by microalgal EPSs from *Cylindrotheca closterium* and *Tetraselmis suecica* biofilms

Julia Mougin^{1,2} · Anne-Sophie Pavaux^{1,2} · Andrea Fanesi² · Julien Lopez³ · Eric Pruvost³ · Freddy Guihéneuf⁴ · Antoine Sciandra³ · Romain Briandet¹ · Filipa Lopes² 

Received: 29 August 2023 / Revised: 20 October 2023 / Accepted: 24 October 2023
© The Author(s), under exclusive licence to Springer-Verlag GmbH Germany, part of Springer Nature 2024

Abstract

In the food industry, successful bacterial pathogen colonization and persistence begin with their adhesion to a surface, followed by the spatial development of mature biofilm of public health concerns. Compromising bacterial settlement with natural inhibitors is a promising alternative to conventional anti-fouling treatments typically based on chemical biocides that contribute to the growing burden of antimicrobial resistance. In this study, three extracellular polymeric substance (EPS) fractions extracted from microalgae biofilms of *Cylindrotheca closterium* (fraction C) and *Tetraselmis suecica* (fraction Ta rich in insoluble scale structure and fraction Tb rich in soluble EPS) were screened for their anti-adhesive properties, against eight human food-borne pathogens belonging to *Escherichia coli*, *Staphylococcus aureus*, *Salmonella enterica* subsp. *enterica*, and *Listeria monocytogenes* species. The results showed that the fraction Ta was the most effective inducing statistically significant reduction for three strains of *E. coli*, *S. aureus*, and *L. monocytogenes*. Overall, EPSs coating on polystyrene surfaces of the different fractions increased the hydrophilic character of the support. Differences in bacterial adhesion on the different coated surfaces could be explained by several dissimilarities in the structural and physicochemical EPS compositions, according to HPLC and ATR-FTIR analysis. Interestingly, while fractions Ta and Tb were extracted from the same microalgal culture, distinct adhesion patterns were observed, highlighting the importance of the extraction process. Overall, the findings showed that EPS extracted from microalgal photosynthetic biofilms can exhibit anti-adhesive effects against food-borne pathogens and could help develop sustainable and non-toxic anti-adhesive surfaces for the food industry.

Key points

- EPSs from a biofilm-based culture of *C. closterium*/*T. suecica* were characterized.
- Microalgal EPS extracted from *T. suecica* biofilms showed bacterial anti-adhesive effects.
- The anti-adhesive effect is strain-specific and affects both Gram – and Gram + bacteria.

Keywords Biofilm · Anti-adhesive coatings · Food-borne pathogens · Microalgae · Exopolysaccharides · Bio-based marine coatings

✉ Romain Briandet
romain.briandet@inrae.fr

✉ Filipa Lopes
filipa.lopes@centralesupelec.fr

¹ Université Paris-Saclay, INRAE, AgroParisTech, Micalis Institute, 78350 Jouy-en-Josas, France

² Laboratoire Génie Des Procédés Et Matériaux (LGPM), CentraleSupélec, Université Paris-Saclay, 91190 Gif-Sur-Yvette, France

³ Laboratoire d, Océanographie de Villefranche LOV, CNRS, Sorbonne Université, UMR 7093, BP 28, 06230 Villefranche-Sur-Mer, France

⁴ Inalve SAS, Nice/Villefranche-Sur-Mer, France

Introduction

In the food industry, biofilm development has been associated with several food-borne disease outbreaks and is considered today as a serious public health concern (Srey et al. 2013). Biofilms are defined as complex microbial communities, including bacteria, attached to a surface and embedded within a self-produced protective matrix extracellular polymeric substances (EPSs). They jeopardize food safety by providing bacteria an ideal protection against disinfectants, which may result in therapeutic failure (Carrascosa et al. 2021). Besides, the emergence and spread of antimicrobial resistance have increased the need for alternative

prophylactic and therapeutic strategies against bacterial food-borne pathogens (Oniciuc et al. 2019). Rather than killing bacteria, more valuable alternatives have thus emerged with the aim of interfering with adhesion (i.e., early step of bacterial colonization) before biofilm maturation and persistence. While biocide-release and chemically active coatings appear to be effective against several unwanted microorganisms, their concern for environment, animal, and human safety limits their use in food-contact materials (Bannister et al. 2019; Mevo et al. 2021). Today, there is thus a shift in the development of antibiofilm surfaces toward non-toxic and sustainable anti-adhesive technologies that are supportive of the *One Health* concept (Destoumieux-Garzón et al. 2018).

In the agri-food sector, microbial-based solutions are increasingly investigated to protect plants or animals for instance with bacterial protective biofilms (Guéneau et al. 2022; Pandin et al. 2017), and another attractive alternative lies within the exploitation of marine microalgae and derivatives, which harbor a wide range of functionalities and bioactive components (Rizwan et al. 2018). Their potential for large-scale cultivations paves the way for the production of high-value compounds such as proteins, lipids, pigments, polyunsaturated fatty acids (PUFAs), or exopolysaccharides with promising economic applications in several branches of industrial markets. In particular, exopolysaccharides are extracellular polysaccharides secreted by microalgae, which can be released into the surrounding environment or bound to the cells forming the major constituents of the EPSs matrix (Delattre et al. 2016). They are complex and various carbohydrate polymers made up of different monosaccharides and frequently associated with non-sugar constituents such as lipids, amino acids, or sulfates attached to their linear or ramified structures. While mostly used for their rheological properties, exopolysaccharides have also been involved in a wide range of biological activities including anti-bacterial, anti-viral, anti-adhesive, antitumor, or immunomodulation (Guzman-Murillo and Ascencio 2000; de Jesus Raposo et al. 2014; Risjani et al. 2021; Talyshinsky et al. 2002; Sun et al. 2009, 2012; Loke et al. 2007). For example, exopolysaccharide extracts from the microalga *Porphyridium marinum* have been used to successfully reduce biofilm formation of the pathogen *Candida albicans* (Gargouch et al. 2021). The attachment of *Vibrio harveyi* and *Salmonella enterica* was significantly inhibited by sulfated polysaccharides from *Chlamydomonas reinhardtii* (Vishwakarma and VL Sirisha., 2020). Similarly, EPSs of *Navicula phyllepta* have shown to harbor anti-biofilm activity against *Flavobacterium* sp., whereas biofilm formation of *Roseobacter* sp. and *Shewanella* sp. was stimulated (Doghri et al. 2017).

Although polysaccharides from algae, bacteria, and mushroom have shown promising anti-biofilm activities

against widespread food-borne pathogens such as *Escherichia coli*, *Staphylococcus aureus*, *Salmonella enterica*, or *Listeria monocytogenes*, no study has investigated microalgal EPSs for wide application in food-contact surfaces (Soliemani et al. 2022; Xu et al. 2020; Abid et al. 2018; Jun et al. 2018; Vunduk et al. 2019). Yet, their high biodegradability and non-toxicity, combined with the opportunity of large-scale production thanks to microalgae cultivation technologies, make them ideal candidates for the development of natural and sustainable anti-adhesive surfaces, with promising applications in food industries (Bernal and Llamas 2012; Rendueles et al. 2013).

Although microalgae have inherent applications, achieving a significant increase in productivity for conventional suspended cultures while reducing operating costs remains a challenge for achieving scaled-up and economically viable production. In order to overcome these drawbacks, biofilm-based cultures have been emerged lately. Among them, an innovative industrialized approach consists of biofilm-based microalgae cultures on rotating cylinders where cells grow attached to a fabric support, forming photosynthetic biofilms embedded in an EPSs matrix (Bernard et al. 2013). Such system allows for a significant decrease of dewatering and harvesting costs, requiring only to scrape the microalgal biomass from the fabric support, instead of time- and cost-consuming harvesting techniques commonly used for planktonic cultures (Mantzorou and Ververidis 2019). In particular, the two microalgae, *Cylindrotheca closterium* and *Tetraselmis suecica*, are known to be able to develop photosynthetic biofilms (Fanesi et al. 2022; Delran et al. 2023), and such a self-organized community might be a source of unexplored bioactive agents to tackle biofouling and bacterial biofilms of health concern. These species have gained a growing interest for their numerous bioactive properties with application in diverse pharmacological and industrial domains, but remain poorly investigated (Sansone et al. 2017; Xiao and Zheng 2016; Guzmán et al. 2019).

The objective of this study was to investigate for the first time the anti-adhesive potential of EPS fractions extracted from microalgae biofilms cultivated in pilot-scale reactors. Early adhesion inhibition was tested using 8 human food-borne bacterial pathogens belonging to *Escherichia coli*, *Staphylococcus aureus*, *Salmonella enterica* subsp. *enterica*, and *Listeria monocytogenes* and quantified by computing the biovolume from confocal laser scanning microscopy (CLSM) images. In order to better understand the mechanisms behind the modification of bacterial adhesion, the physicochemical properties of the different EPS fractions were characterized using attenuated total reflectance Fourier transform infrared (ATR-FTIR) spectroscopy, high-performance liquid chromatography (HPLC), and contact angle measurements.

Material and methods

Preparation of microalgae extracts

Cylindrotheca closterium AC170 and *Tetraselmis suecica* AC254 from the Algotank-Caen culture collection (University of Caen, France) were cultivated as biofilms using a pilot patented rotating system (WO 2021180713A1) (Penaranda et al. 2023; Bernard et al. 2013). *T. suecica* biomass was cultured by the company Inalve (Nice, France) under natural light and photoperiod during 250 days, from September 2020 to May 2021; while *C. closterium* was cultured by the Laboratoire d'Océanographie de Villefranche (LOV, Villefranche-sur-Mer) for approximately 100 days, from April to July 2022. The rotating biofilm systems were placed in a pond filled with filtered seawater (1, 0.5, and 0.2 μm) treated by UV radiation (BIO-UV, UV-C 254 nm, 225 mj/cm^2) and operated within a greenhouse at room temperature. Water temperature in tanks ranged from 10 to 26 $^{\circ}\text{C}$ (mean 16.7 ± 3.5 $^{\circ}\text{C}$) for *T. suecica* and from 20 to 35 $^{\circ}\text{C}$ (mean 25.0 ± 2.0 $^{\circ}\text{C}$) for *C. closterium*. Pulse of nutrients was performed every 7 days using a modified f/2 medium, double strengthened with N and P, with a supplement of silicate for *C. closterium* (Guillard 1975; Ryther and Guillard 1962). Every 14 or 21 days, microalgae biomass from the biofilms was harvested by scraping the surface of the different pilots, and the medium was renewed.

Extracellular polymeric substances (EPSs, Crude extracts) from *C. closterium* and *T. suecica* biofilms were extracted in water with agitation for 1 h at room temperature followed by low-speed filter-centrifugation with 1–5- μm filter fiber at 1000 rpm for 10 min (Fig. 1). The crude extracts were then processed as follows: (i) *C. closterium* soluble EPSs from crude extract were directly obtained by ultrafiltration at 5 kDa in order to concentrate the overall EPS fraction

(Fraction C; IAVC2; solubility > 90% from 1 to 10 $\text{g}\cdot\text{L}^{-1}$ in Milli-Q water) and eliminate the salts by diafiltration using a SIVALAB ultrafiltration pilot equipped with 5 kDa ceramic membranes (Nyons, France); (ii) *T. suecica* insoluble EPS fraction from crude extract was obtained after high-speed centrifugation with CLARA 20 (GEA) (11,130 $\times g$; 30 min) from the pellet (Fraction Ta; IAVT2_a; solubility of 33% from 1 to 10 $\text{g}\cdot\text{L}^{-1}$ in Milli-Q water); the clarified supernatant obtained was then ultra-filtrated at 5 kDa in order to concentrate the soluble EPS (Fraction Tb; IAVT2_b; solubility of 87% from 1 to 10 $\text{g}\cdot\text{L}^{-1}$ in Milli-Q water) and remove the salts as previously described. Extracts were freeze-dried using a BUCHI LyovaporTM L-200 Freeze Dryer and stored at 4 $^{\circ}\text{C}$ until used. In summary, one fraction, Fraction C, was obtained from *C. closterium*, and two fractions, Fractions Ta and Tb, were extracted from *T. suecica* (Fig. 1).

Bacterial strains and growth conditions

A total of 8 isolates belonging to *Escherichia coli* (SS2, CIRMBP-0223, and CIRMBP-0248), *Staphylococcus aureus* (HG003), *Salmonella enterica* subsp. *enterica* (Serotype Infantis NCTC 35616 and Serotype Enteritidis CCUG 6678), and *Listeria monocytogenes* (ScottA and EGD-e) were used as human model pathogens (Table 1). Each strain was previously modified to express the green fluorescent protein (GFP), as described in Table 1. In prior experiments, *E. coli* and *S. enterica* subsp. *enterica* isolates were sub-cultured on Tryptic Soy Agar (TSA) supplemented with ampicillin at 100 $\mu\text{g}\cdot\text{mL}^{-1}$ to maintain the plasmid carrying the *gfp* gene, while for *S. aureus* and *L. monocytogenes* isolates, erythromycin at 5 $\mu\text{g}\cdot\text{mL}^{-1}$ was used. After incubation for 8 h at 37 $^{\circ}\text{C}$, a single colony forming unit (CFU) expressing the GFP (observation at UV light) was selected and cultured in 5 mL of Tryptic Soy Broth (TSB), overnight at 37 $^{\circ}\text{C}$.

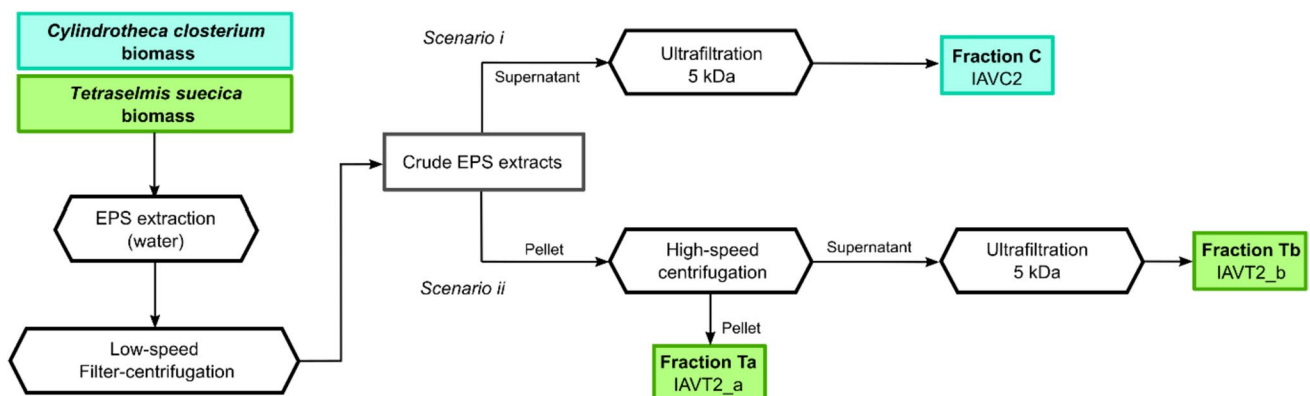


Fig. 1 Extraction process and fractionation of crude exopolysaccharides (EPSs) from *Cylindrotheca closterium* and *Tetraselmis suecica* biofilms. Fraction C corresponds to an extract from *C. closterium*, while fractions Ta and Tb were extracted from *T. suecica*

Table 1 List of bacterial strains used in this study

Strain ID	Species	Origin	Plasmid	Reference
SS2	<i>Escherichia coli</i>	Industry	pCM11_sGFP	(Gomes et al. 2017)
CIRMBP-0223	<i>Escherichia coli</i>	Chicken, trachea	pCM11_sGFP	(Guéneau et al. unpublished)
CIRMBP-0248	<i>Escherichia coli</i>	Chicken, intestine	pCM11_sGFP	
HG003	<i>Staphylococcus aureus</i>	NCTC 8325 derivative isolated from human	pAH13	(Malone et al. 2009)
NCTC 6678	<i>Salmonella enterica</i> subsp. <i>enterica</i> Serotype Enteritidis	Cow	pCM11_sGFP	(Guéneau et al. unpublished)
CCUG 35612	<i>Salmonella enterica</i> subsp. <i>enterica</i> Serotype Infantis	Pasta	pCM11_sGFP	
ScottA	<i>Listeria monocytogenes</i>	Clinical isolate from a food-borne listeriosis outbreak	pCM11_sGFP	(Lauderdale et al. 2010)
EGD-e	<i>Listeria monocytogenes</i>	Rabbit	pNF8	(Habimana et al. 2009)

Adhesion assay

Early adherence assay to a polystyrene surface was carried out in 96-well microtiter plates (μ clear, black, Greiner Bio-One, Frickenhausen, Germany). The surface of the wells was coated with the different fractions C, Ta, and Tb, by adding 150 μ L of each extract diluted at 2 mg.mL⁻¹ in sterile TSB and incubating at 4 °C during 24 h. The solution was then discarded prior the addition of bacteria.

For each tested bacterial strain, a GFP expressing colony from a 24 h-TSA culture with antibiotic was selected and grown in TSB without antibiotic, at 37 °C for 8 h with shaking. Bacterial solution was then diluted to 50% in fresh TSB medium, and 200 μ L was deposited in each coated well. Bacteria were cultivated for 1 h at 37 °C under static conditions. To safeguard against any influence from growth-related factors, we deliberately chose a time point before the onset of the exponential phase for all tested strains; this decision was guided by the results obtained from bacterial growth curves analysis (data not shown), thus ensuring that the observed effects could be solely attributed to adhesion. After incubation, non-adhered bacteria were removed, and 200 μ L of fresh media was added prior to microscopic observation. Blank control consisted of sterile TSB medium, and 100% biofilm control consisted of bacterial surface accumulation without coating.

Biofilm observation was performed using a Leica HCS-SP8 Confocal Laser Scanning Microscope (CLSM, LEICA Microsystems, Wetzlar, Germany) at the INRAe MIMA2 imaging platform (doi.org/<https://doi.org/10.15454/1.5572348210007727E12>). An argon laser set at 30% intensity was used for excitation at 488 nm, and the emitted fluorescence was recorded between 500 and 550 nm. A $\times 63$ water immersion objective lens (Leica HC PL APO CS2) was used with a 512 \times 512-pixel definition and a bidirectional acquisition speed of 600 Hz. For 3D stack acquisition, a 1- μ m axial resolution was applied. The CLSM images were reconstructed

into 3D images using IMARIS ver. 9.3.1 (Bitplane AG, Zurich, Switzerland), and biofilm biomass was estimated by calculating the biovolume (μm^3 . μm^{-2}). A total of 3 replicate wells were performed for each experiment, and 3 random CLSM acquisitions per well were recorded. Four independent experiments (i.e., four different microplates) were carried out ($n = 12$ for each condition, with 36 CLSM acquisitions per condition).

Characterization of microalgae extracts and coated surfaces

Chemical analysis

Dry matter, ash, protein, sulfate, and carbohydrate composition of microalgae extracts were determined by the CEVA (Centre d'Etude et de Valorisation des Algues, Pleubian, France) according to previously reported methods. The dry weight (DW) was evaluated according to the reduction of sample weight after 24 h at 103 °C. Ash content was determined gravimetrically after combustion at 550 °C for 12 h, following a reference procedure (AFNOR, standard NF ISO 5984), in order to estimate the efficiency of the desalting step. Protein content was estimated using the standard Kjeldahl nitrogen analysis; an N-to-protein conversion factor of 6.25 was used (Marinho-Soriano et al. 2006). Sulfate content was determined using the turbidimetric method of barium sulfate (BaSO₄) (Tabatabai 1974) in order to estimate the proportion of sulfated polysaccharides. Neutral sugar, mannitol, and uronic acid composition was evaluated by high-performance liquid chromatography (HPLC) analysis after controlled methanolysis in MeOH-HCl, using an absorbosphere RP18 column (RP18, 5 μ m, 4.6 \times 250 mm GraceSmart, Deerfield, IL, USA) as described by Quémener et al. (2000). Chromatographic peaks were identified according to high purity reference standards.

ATR-FTIR spectroscopy

Attenuated total reflexion Fourier transform infrared (ATR-FTIR) spectroscopy was performed as previously described by Fanesi et al. (2019). Briefly, ATR-FTIR spectra were obtained using a PerkinElmer Spectrum-two spectrometer (PerkinElmer, Waltham, MA, USA). Spectra were recorded in reflectance mode between 4000 and 400 cm^{-1} using 32 accumulations at a spectral resolution of 4 cm^{-1} . Spectra were baselined using the rubber band algorithm and normalized at the Amide I band.

Contact-angle assay

After coating the supports with the different fractions, surface hydrophobicity was measured by static contact-angle measurements (5 μL drop of distilled water) with an automatic drop tensiometer (Tracker Teclis/IT Concept, France) as described by Li et al. (2023). Angle values were calculated using the ImageJ 1.53t software with the Contact-Angle plugin and were the average of 6 measurements.

Calculation and statistical analysis

The percentage of bacterial surface accumulation was determined according to the biovolume ($\mu\text{m}^3 \cdot \mu\text{m}^{-2}$) obtained from CLSM stacks as follows:

$$\text{Biofilm adhesion(\%)} = 100 \times \frac{\text{Biovolume}_{\text{Sample}}}{\text{Biovolume}_{100\% \text{control}}} \quad (1)$$

The 100% control corresponds to the biovolume of bacterial biomass adhered on surfaces without coating (untreated bacteria). Statistical analyses were performed using RStudio ver. 4.2.0 software (R Core Team 2013). Differences in bacterial adhesion biomass compared to the control were determined using a one-way analysis of variance (ANOVA); after that, normality and homoscedasticity of the distribution hypothesis were verified, followed by a Dunnett post hoc test. A post hoc test was performed using the DescTools package ver. 0.99.47 (Signorell et al. 2019). The differences were considered statistically significant at p -value < 0.05. Graphics were drawn using the ggplot2 package ver. 3.3.6 (Wickham 2016).

Results

Adhesion assay

Overall, our results show no difference in bacterial adhesion between the control and the fractions C and Tb, while 3 bacterial strains exhibited lower adhesion capacity for the fraction Ta (Fig. 2A). For the latter, significant differences

were observed for ScottA, where only $41.9 \pm 17.9\%$ of adhered bacterial biovolume was measured, compared to the control (ANOVA, Dunnett test; p -value = 0.0292). Similarly, only 59.9 ± 17.0 and $60.0 \pm 19.5\%$ of *S. aureus* HG003 and *E. coli* SS2 bacterial biovolume, respectively, adhered to the fraction Ta (ANOVA, Dunnett test; p -value = 0.0065 and 0.024, respectively).

CLSM observations displayed in Fig. 2B showed that most of the strains adhered to the control surface in a homogeneous way, with aggregates observed for *E. coli* SS2 and *S. enterica* subsp. *enterica* CCUG 35616/NCTC 6678. However, adherence to the surfaces coated with the fraction C, Ta, and Tb highlighted different 3D configurations for *S. aureus* HG003, exhibiting the clustering of specific aggregates and regions of no adhesion. Similarly, fractions Tb induced different 3D adhesion patterns for *E. coli* CIRMBP-0248 and *L. monocytogenes* EGD-e compared to the control, as well as fraction Ta for both strains of *L. monocytogenes*.

Physicochemical characterization of the microalgae extracts

In order to unravel the dissimilarities in structural and physicochemical composition that may potentially explain the difference in bacterial adhesion, microalgal extracts were analyzed for dry matter, ash, sulfate, protein, and carbohydrate contents. The chemical composition of the microalgal EPS fractions C, Ta, and Tb is given in Table 2.

Fractions Ta and Tb were mostly composed of carbohydrates (35.1 and 30.5% DW, respectively), while fraction C showed a high content of proteins (37.0% DW), followed by carbohydrates (30.6% DW). Sulfate content was relatively low for fractions C and Ta (1.0 and 3.7% DW, respectively), whereas fraction Tb exhibited a higher concentration (12.7% DW). Overall, total carbohydrate content was similar between the 3 fractions ranging from 30.5 to 35.1% DW, while divergences were observed in compositions.

Fraction C was mainly constituted by glucose representing 35.6% of total carbohydrates, while fraction Ta harbored 69.3% of Kdo and fraction Tb was mainly constituted of 59.0% of galactose and 23.4% of Kdo. A high content of glucuronic acid (19.6%) was measured in fraction C, and fraction Ta harbored the greatest content of galacturonic acid (10.5%). Kdo was not present in fraction C, and fraction Ta did not contain rhamnose and fucose; none of the fractions comprised mannitol.

The FTIR spectroscopy analysis was then performed to evaluate the differences between the chemical structure of the different fractions according to the band assignments in literature (Murdock and Wetzel 2009; Scarsini et al. 2021; Fanesi

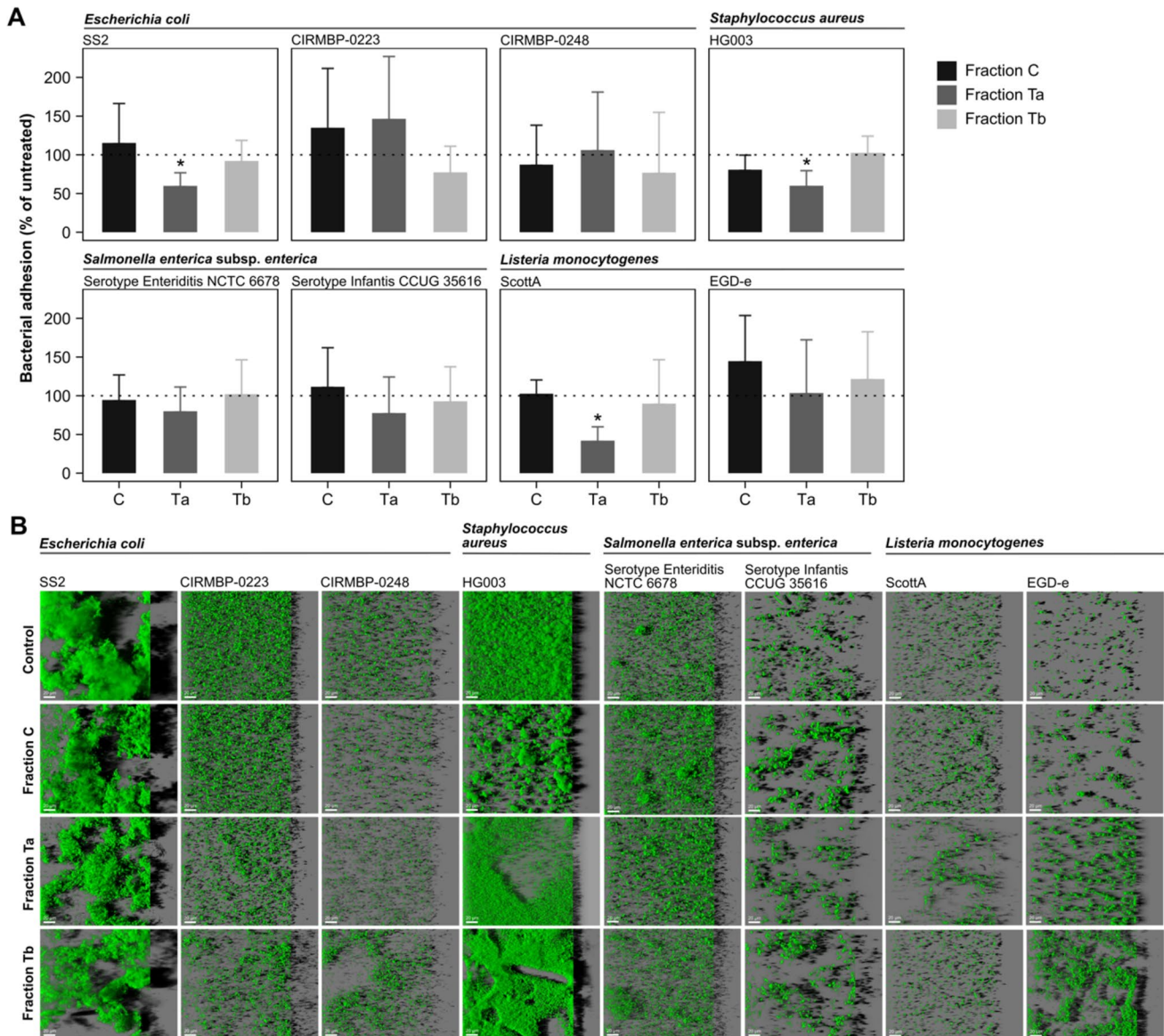


Fig. 2 Bacterial adhesion inhibition of the different tested strains cultured for 1 h at 37 °C on 96-well microtiter plates after coating with the different microalgae extracts: fractions C, Ta, and Tb. **A** Percentage of bacterial adhesion was determined according to the GFP-tagged biofilm biovolume ($\mu\text{m}^3 \cdot \mu\text{m}^{-2}$) and reported relative to the control defined as 100% (untreated bacteria) and sterility control wells defined as 0%. The horizontal bar denotes the 100% control for reference. Vertical bars represent means \pm standard deviations (3 bio-

logical replicates for each of the 4-independent assays; $n=12$). The asterisk (*) symbols stand for significantly different values compared to the 100% control (ANOVA, Dunnett test; p -value < 0.05). **B** Representative IMARIS easy 3D projections, depicting the GFP-tagged CLSM biofilm observation at a magnification of $\times 63$. The shadows on the right represent the virtual lateral biofilm projection of the submerged biofilm. White scale bars represent 20 μm

et al. 2019; Soto-Vásquez et al. 2022). As displayed in Fig. 3 and Table 3, the FTIR spectrum of EPS fractions extracted from *C. closterium* and *T. suecica* showed several dissimilarities. Overall, in each fraction, a broad band of vibration was detected between 3000 and 3500 cm^{-1} attributed to the stretching vibration of O–H and N–H groups, followed by a weak signal between 2800 and 2950 cm^{-1} corresponding to C–H, CH_2 , and CH_3 stretching vibrations (Table 3). The presence of a vibration band at 1635 cm^{-1} (Fig. 3, Table 3

[2]) is associated with the stretching of C=O (Amide I), and the presence of a peak at 1545 cm^{-1} (Fig. 3, Table 3 [3]) is characterized to the bending of N–H and stretching of C–N bonds (Amide II). However, the fraction Ta presents a slightly shifted peak at 1605 cm^{-1} (Fig. 3, Table 3 [2]) compared to those from the fractions C and Tb. The bands at 1405 cm^{-1} (Fig. 3, Table 3 [4]) of the different fractions are related to the stretching vibration of C–O bonds, while those around 1245 cm^{-1} (Fig. 3, Table 3 [5]) may correspond to

Table 2 Average chemical composition of the different microalgae extracts: fraction C, Ta, and Tb. Concentrations are expressed in g (100 g)⁻¹ dry weight (DW), except for carbohydrate concentrations which are expressed relative to the total carbohydrate contents. Abbreviation: *Kdo* 3-deoxy-d-manno-oct-2-ulosonic acid

	Fraction C	Fraction Ta	Fraction Tb
Dry weight DW g (100 g) ⁻¹	90.8	94.4	93.1
Ash (% DW)	12.1	29.7	21.9
Sulfate (% DW)	1.0	3.7	12.7
Proteins (% DW)	37.0	22.1	25.4
Total carbohydrates (% DW)	30.6	35.1	30.5
Carbohydrates composition (% total carbohydrates)			
Galactose	16.7	8.9	59.0
Glucose	35.6	8.6	5.1
Mannose	2.3	1.3	1.6
Rhamnose	13.7	0.0	2.1
Fucose	7.5	0.0	2.6
Kdo	0.0	69.3	23.4
Galacturonic acid	4.6	10.5	4.5
Glucuronic acid	19.6	1.3	1.8
Mannitol	0.0	0.0	0.0

S=O or P=O bonds. Besides, when comparing the intensity between spectra, the fraction Tb showed higher intensity of the vibration band associated with S=O or P=O between 1300 and 1200 cm⁻¹ than for the fraction C and Ta. Vibration bands between 1200 and 950 cm⁻¹ (Fig. 3, Table 3 [6]), often associated with the stretching vibration of C–O–C, showed various deformations and thus highlight high dissimilarities between the 3 spectra. Fraction C presented distinctive peaks around 1088 cm⁻¹ (Fig. 3, Table 3 [7]) characteristic of silica; while fraction Ta presented a distinctive pattern with a peak around 1015 cm⁻¹ (Fig. 3, Table 3 [8]) characteristic of starch and cellulose.

Contact-angle analysis highlighted a decrease in the hydrophobicity of the surface coated with the different fractions, with angle values corresponding to 25.7 ± 4.7° for fraction C, 31.1 ± 6.4° for fraction Ta, and 39.7 ± 6.3° for fraction Tb (*n* = 6). The non-coated substrate exhibited an angle of 46.2 ± 4.5°.

Discussion

The objective of this study was to investigate the anti-adhesive properties of EPS constituents extracted from microalgal photosynthetic biofilms, with the aim of developing

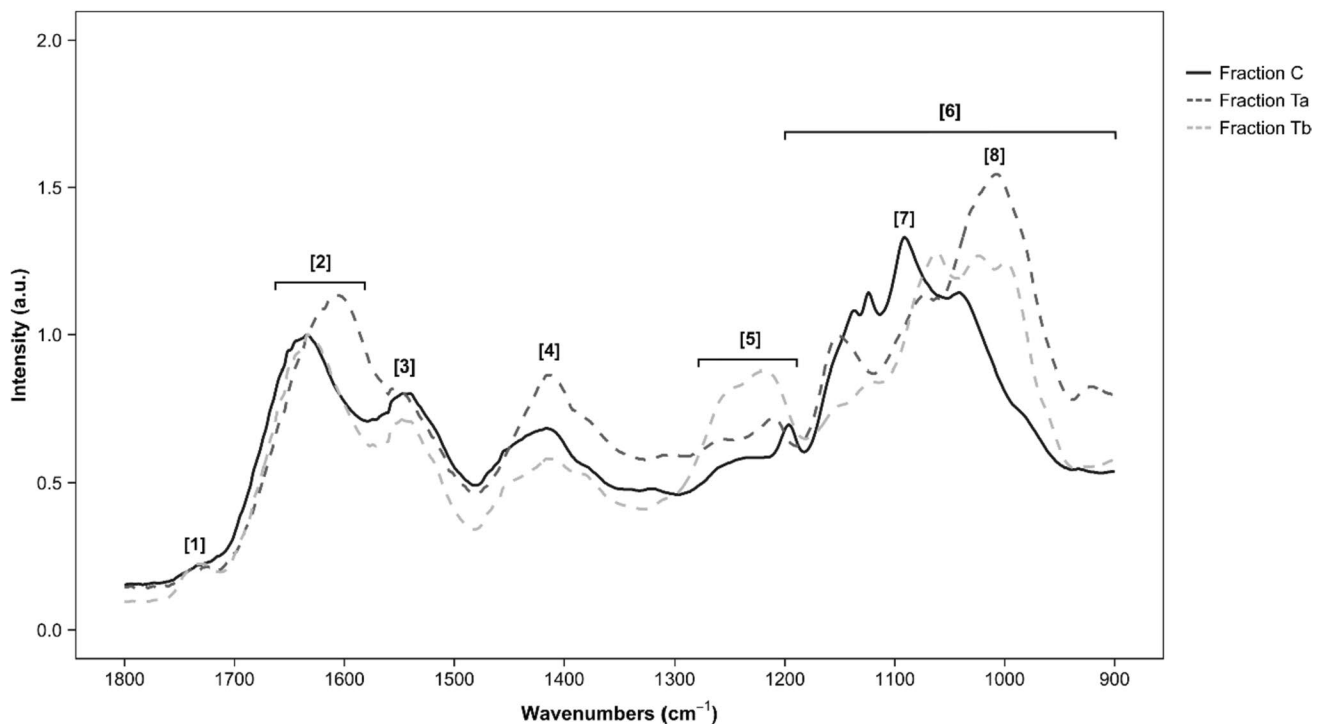


Fig. 3 Normalized ATR-FTIR spectra of EPSs extracted from the microalgae *C. closterium* (Fraction C) and *T. suecica* (Fractions Ta and Tb). Spectra were normalized using the Amide I band, selected

as an internal reference to facilitate visual comparisons. The numbers [#] correspond to the bands # in the Table 3. Only the wavenumbers from 1800 to 900 cm⁻¹ are represented. a.u., arbitrary units

Table 3 Range of FTIR band from the spectra of the microalgal EPS extracts fraction C, Ta, and Tb, as well as their potential assignments according to literature. The bands # correspond to the numbers [#] in Fig. 3. ν = symmetric stretching, ν_{as} = asymmetric stretching, δ = sym-

metric deformation. Band assignments were determined according to Murdock and Wetzel (2009). + stands for presence and – stands for absence

Results	Tentative band assignments from literature			Potential functional group	Presence/absence in EPS fractions		
	Band zone #	Wavenumbers in this study (cm^{-1})	Wavenumbers in literature (cm^{-1})		Vibration type	C	Ta
/	3400–3100	3400–3300	$\nu(\text{O}-\text{H})$ $\nu(\text{N}-\text{H})$	Water Proteins	+	+	+
/	2950–2800	2970–2850	$\nu_{as}(\text{CH}_3)$ $\nu_{as}(\text{CH}_2)$ $\nu(\text{CH}_2, \text{CH}_3)$	Methyl and methylene groups of lipids	+	+	+
[1]	1730	1745–1734	$\nu(\text{C}=\text{O})$ of esters	Membrane lipids, fatty acids	+	+	+
[2]	1635	1655–1638	$\nu(\text{C}=\text{O})$	Proteins (Amide I)	+	–	+
	1605				–	+	–
[3]	1545	1545–1540	$\delta(\text{N}-\text{H})$ $\nu(\text{C}-\text{N})$	Proteins (Amide II)	+	+	+
[4]	1405	1460–1392	$\nu(\text{C}-\text{O})$	Carboxyl group	+	+	+
[5]	1275–1185	1255–1250	$\nu_{as}(\text{S}=\text{O})$	Sulfate group	+	+	+
		1244–1230	$\nu_{as}(\text{P}=\text{O})$	Nucleic acid, Phosphorylated sugars			
[6]	1180–950	1200–950	$\nu(\text{C}-\text{O}-\text{C})$ $\nu_{as}(\text{P}=\text{O})$	Polysaccharides Nucleic acids	+	+	+
[7]	1088	1100–1060	$\nu(\text{Si}-\text{O})$	Biogenic silica	+	–	–
[8]	1015	1100–900	$\nu(\text{C}-\text{O})$	Starch/cellulose	–	+	–

non-toxic and sustainable anti-adhesive surfaces for wide application in food-contact materials. Anti-adhesion properties and chemical composition of 3 EPS fractions extracted from 2 species of microalgae *Cylindrotheca closterium* (fraction C) and *Tetraselmis suecica* (fractions Ta and Tb) were characterized. Anti-adhesion effect was investigated using 8 human food-borne pathogens belonging to *Escherichia coli*, *Staphylococcus aureus*, *Salmonella enterica* subsp. *enterica*, and *Listeria monocytogenes*. Overall, exopolysaccharides were the major constituents of the different extracts, in particular fractions Ta and Tb. Fractions C, Ta, and Tb exhibited different anti-adhesion properties that may be explained by several dissimilarities observed in structural and chemical compositions. Bacterial exposure to a surface coated with the fraction Ta generated lower early adherence capacity for 3 strains of *E. coli*, *S. aureus*, and *L. monocytogenes*, while exposure to fractions C and Tb exhibited no difference with respect to the control.

Fractions Ta exhibited the greatest anti-adhesion properties for both Gram-negative and Gram-positive bacteria

Coating with the different fractions induced distinct adhesion patterns and 3D conformations revealed by the GFP-tagged biofilm observations using CLSM. Our results showed that one Gram-negative strain belonging to *E. coli* and two Gram-positive strains belonging to *S. aureus* and *L. monocytogenes* displayed low adherence capacity for fraction Ta,

while adherence of *Salmonella enterica* subsp. *enterica* was similar to the control. More precisely, fraction Ta exhibited around 40% biovolume inhibition of adhered bacteria for *E. coli* SS2 and *S. aureus* HG003 and 58% of biovolume inhibition of adhered bacteria for *L. monocytogenes* ScottA. The results demonstrate that the effect is strain-specific instead of species-specific and that the anti-adhesion activity impacts both Gram-negative and Gram-positive bacterial pathogens.

Although not fully understood, various mechanisms could explain the inhibition of bacterial adhesion including the modification of the chemical and physical properties of the surface, which may weaken the cell-surface contacts (Zheng et al. 2021). Surface topography is also known to influence initial cell-surface interactions, along with surface roughness commonly linked to the modification of bacterial attachment and 3D conformations. Polysaccharides act as biosurfactants affecting the surface hydrophobicity and electrostatic charges. Indeed, our results from contact-angle analysis indicated that the 3 fractions were able to alter the wettability of the surface by increasing its hydrophilicity. It is frequently admitted that hydrophilic materials are less susceptible to bacterial adhesion than hydrophobic ones (Fajó et al. 2023), whereas some contradictory opinions do exist (Zhang et al. 2013). In particular, Valle et al. (2006) demonstrated that polysaccharides secreted by *E. coli* induced physicochemical surface alterations, which further reduced adhesion and biofilm formation of nosocomial pathogens. Coating of glass surfaces with the culture supernatant decreased the water-slide interfacial energy, suggesting a hydrophilic character.

Similarly, they demonstrated an anionic nature of the supernatants which may be involved in the antiadhesive properties of the fractions. Bacterial cell walls are negatively charged at neutral pH, and adherence to anionic surface will thus be compromised by the electrostatic repulsion forces. That is why anionic polysaccharides with hydrophilic characteristics have been highly investigated for their high potential in the development of anti-adhesive surfaces (Junter et al. 2016). In addition, Gadenne et al. (2015) have also highlighted the role of molecular weight (MW) of polysaccharides and their immobilization protocol in the anti-adhesive effect of the coated surface. The difference in adhesive capacity of coated polysaccharides with distinct MW appeared to follow a parabolic behavior, leading to distinct layer conformations. For instance, Dong et al. (2011) demonstrated that surfaces coated with polyethylene glycol (PEG) at a MW of 2000 harboured an optimal antifouling ability compared to PEG with higher and lower MW.

Exopolysaccharides may not only impact cell-surface interactions and the initial adhesion, but they could also interfere with cellular interactions along with the biofilm development, maturation, and dispersal (Valle et al. 2006; Jiang et al. 2011). For instance, the exopolysaccharide A101 purified from the culture supernatant of *Vibrio* sp. has the ability to disrupt the established biofilm and aggregates of bacterial pathogens without affecting bacterial growth, suggesting that A101 is able to interfere with cell–cell interactions (Jiang et al. 2011). Another study indicated that anti-biofilm activity of the exopolysaccharides from *Lactobacillus acidophilus* was associated with changes in gene expression patterns of *E. coli* related to the production of curli adhesive surface fibers and chemotaxis, which are known to affect biofilm architecture (Kim and Kim 2009).

The modification of properties such as wettability and electrostatic charge, related to the antiadhesive effect, depends on the chemical composition of the coated surface associated with the EPSs. That is why we further investigated the chemical and structural composition of the EPS fractions to better understand the mechanisms driven by the observed adhesion inhibition.

EPS extracts showed different chemical and structural compositions

The chemical and structural analysis of the different fractions highlighted great structural diversity and complexity in EPS fractions C, Ta, and Tb, with a high content of polysaccharides. Both ATR-FTIR and HPLC are advanced analytical methods widely used for the characterization of EPSs, providing valuable insights into their physicochemical structures and compositions. Thanks to the ATR-FTIR analysis performed on a global mixture, we unveiled the complex and heterogeneous character of the different fractions. Then, the HPLC

analysis based on the separation of the different substances allowed to characterize individually the compounds within the mixtures, which further helped in unveiling the oligosaccharide composition.

Fraction C extracted from the diatom *C. closterium* consisted of a high content of proteins and carbohydrates, with glucose being the most abundant. Interestingly, the major form of storage polysaccharide of diatom, such as *C. closterium*, is chrysolaminarin, which degradation produces glucose (Wagner et al. 2017). Moreover, ATR-FTIR spectral analysis revealed vibrations that are characteristic of silica. Those results are in agreement with previously reported literature, in which diatom exhibited a characteristic FTIR pattern due to the presence of silica frustule (cell wall) (Murdock and Wetzel 2009).

Fraction Tb exhibited the highest concentration of sulfate, which may indicate the potential presence of sulfated exopolysaccharides. Interestingly, several bacterial pathogens had shown affinity for sulfated glycoconjugates found on the surface of eukaryotic epithelial cells, and the use of agonist compounds such as sulfated exopolysaccharides may help in reducing bacterial adhesion by a competition process (Ofek et al. 2003). For instance, Guzman-Murillo and Ascencio (2000) have shown that microalgal sulfated exopolysaccharides can be effectively used to reduce human pathogen adhesion *Helicobacter pylori* to the HeLa S3 cell line, as well as the fish pathogens adhesion *Aeromonas veronii*, *V. campbellii*, *V. ordalii*, and *Streptococcus saprophyticus*, to spotted sand bass primary tissue culture cells. Similarly, glucuronic acid-enriched polysaccharides help in blocking the adhesion of *H. pylori* on human stomach tissue (Wittschier et al. 2007), and here fraction C, containing the highest amount of glucuronic acid might be investigated for its therapy potential. Though the presence of uronic acids and sulfated polysaccharides in fractions Tb and C cannot explain our data, these extracts should be further studied for their possible anti-adhesive effectiveness and use in human therapies.

Both fractions Ta (rich in insoluble scale structure) and Tb (rich in soluble EPS) contained 3-deoxy-d-manno-oct-2-ulosonic acid (Kdo), with fraction Ta exhibiting the highest content, along with a FTIR spectral pattern associated with starch. Those results are similar to those previously obtained in the literature (Kermanshahi-Pour et al. 2014; Delran et al. 2023). Indeed, the cell wall of *T. suecica* is described as being composed of different layers composed of carbohydrates (up to 45% DW of starch) and proteins, forming a complex network and providing a more resistant cell structure (Delran et al. 2023). This network contains mainly galactose, xylose, rhamnose, mannose, and arabinose as well as up to 5% DW of the rare sugars Kdo (Kermanshahi-Pour et al. 2014). All these compounds form a strong and relatively rigid scale structure of the cell wall. Depending on the culture conditions, it has been observed that *T. suecica*

cell wall can be formed by 5 layers (Azma et al. 2010). It should be pointed out that Kdo sugar is a core element of bacterial lipopolysaccharides (LPSs) which have been found in the outer membrane of numerous Gram-negative bacteria, including human pathogens (Stead et al. 2005; Okan et al. 2013). Interestingly, it has a high potential in pharmaceutical applications, due to its immunostimulant and as a therapeutic target potential (Cipolla et al. 2010; Cloutier and Gauthier 2020). Whether the high amount of Kdo in fraction Ta may explain the greater inhibition effect of early bacterial adhesion is uncertain and needs further investigations, although it is clear that *T. suecica* is a high-value species which need to be further explored for its EPS biosynthesis, in particular Kdo production, with potential economical and pharmaceutical interests.

Future outlooks on the application of microalgal EPSs as anti-adhesive surfaces

Our data clearly shows that EPSs extracts from *T. suecica* microalgae biofilms (Ta) have anti-adhesive properties against some Gram-positive and Gram-negative bacteria. Microalgae biofilms can therefore represent an important source of natural anti-fouling compounds.

Composition of EPSs is significantly affected by the production conditions including microalgal strains, culture conditions, and extraction process (Costa et al. 2021). First, we demonstrated that two fractions—fractions Ta and Tb—originated from the same microalgae cultures had distinct antiadhesive properties, confirming that the extraction process plays a key role in the isolation of components of interest. Second, this study helps characterising EPSs from microalgae biofilm-based cultures which are barely studied compared to those from planktonic cells. Several studies highlighted an increased polysaccharide yield and significant differences in chemical composition among planktonic and biofilm bacterial cultures (Kives et al. 2006). We may thus speculate that new compounds at high productivity can be produced with biofilm-based cultures. In addition, it has been shown that the combination of different stages including optimal growth conditions that stimulate biomass production, along with stress-related conditions that favor polysaccharide production, enable to achieve higher yields of microalgal polysaccharides (Cruz et al. 2020). Besides increased productivity, such techniques may also favor the production of unique bioactive components. Indeed, crude extracts from the diatom *Leptocylindrus* sp. cultured in stress conditions (N-starvation) showed acute anti-biofilm activity against *Staphylococcus epidermidis*, while no effect was observed when no stress was applied (Lauritano et al. 2016).

In conclusion, in this study, the physicochemical and biological-activity relationship of EPSs fractions extracted

from biofilm-based cultures of *C. closterium* (fraction C) and *T. suecica* (fractions Ta and Tb) was characterized. Fraction Ta harbored the greatest anti-adhesive properties against food-borne pathogens, which could be explained by structural and physicochemical peculiarities. This effect was strain-specific and affected both Gram-negative and Gram-positive bacteria. Further work must be carried out to identify compound(s) responsible for its antiadhesive behavior, along with the interaction mechanisms between bacteria and anti-fouling compound(s). Its/their in-depth characterization as well as assessment of toxic susceptibility and biodegradability will be crucial for application in food-contact materials. Besides the development of sustainable and non-toxic anti-adhesive surfaces for food industries, such compounds have inherent wide applications, ranging from marine, agricultural, and industrial equipment, including ship hulls and aquaculture sea-cages, to biomedical devices such as biosensors and implants (Banerjee et al. 2011).

Acknowledgements We are grateful to Raphael Marie and Amélie Talec from the Laboratoire d'Océanographie de Villefranche (LOV) for their help in setting up biofilm-based microalgal cultures. The authors are also grateful to the French Antibioideal network of the Promise PPR antibioresistance ANR program for stimulating scientific exchanges.

Author contribution JM wrote the original draft; JM, ASP, and AF analyzed the data; ASP and AF conducted experiments; JL, EP, FG, and AS contributed to the microalgal biomass and fractions; RB and FL conceived and designed research. JM, AF, JL, FG, AS, RB, and FL reviewed and edited the manuscript; all authors read and approved the manuscript.

Funding This work was funded by the French ANR PhotoBiofilmExplorer program.

Data availability The data analyzed in this study are within the paper or related references.

Declarations

Ethical approval This article does not contain any studies with human participants or animals performed by any of the authors.

Conflict of interest The authors declare no competing interests.

References

- Abid Y, Casillo A, Gharsallah H, Joulak I, Lanzetta R, Corsaro MM, Attia H, Azabou S (2018) Production and structural characterization of exopolysaccharides from newly isolated probiotic lactic acid bacteria. *Int J Biol Macromol* 108:719–728. <https://doi.org/10.1016/j.ijbiomac.2017.10.155>
- Azma M, Mohamad R, Rahim RA, Ariff AB (2010) Improved protocol for the preparation of axenic culture and adaptation to heterotrophic cultivation. *The Open Biotechnol J* 4:36–46. <https://doi.org/10.2174/1874070701004010036>
- Banerjee I, Pangule RC, Kane RS (2011) Antifouling coatings: recent developments in the design of surfaces that prevent fouling by proteins, bacteria, and marine organisms. *Adv Mater* 23:690–718. <https://doi.org/10.1002/adma.201001215>

- Bannister J, Sievers M, Bush F, Bloecher N (2019) Biofouling in marine aquaculture: a review of recent research and developments. *Biofouling* 35:631–648. <https://doi.org/10.1080/08927014.2019.1640214>
- Bernal P, Llamas MA (2012) Promising biotechnological applications of antibiofilm exopolysaccharides. *Microb Biotechnol* 5:670. <https://doi.org/10.1111/j.1751-7915.2012.00359.x>
- Bernard O, Sciandra A, Pruvost E, and Lopes F (2013) Method and unit for producing microalgae. Patent WO2015007724
- Carrascosa C, Raheem D, Ramos F, Saraiva A, Raposo A (2021) Microbial biofilms in the food industry—a comprehensive review. *Int J Environ Res Public Health* 18:2014. <https://doi.org/10.3390/ijerph18042014>
- Cipolla L, Gabrielli L, Bini D, Russo L, Shaikh N (2010) Kdo: a critical monosaccharide for bacteria viability. *Nat Prod Rep* 27:1618–1629. <https://doi.org/10.1039/C004750N>
- Cloutier M, and Gauthier C (2020) 3-deoxy-D-manno-oct-2-ulosonic acid (Kdo) derivatives in antibacterial drug discovery. in, *Carbohydrates in drug discovery and development* (Elsevier). p 155–212. <https://doi.org/10.1016/B978-0-12-816675-8.00004-X>
- Costa JAV, Lucas BF, Alvarenga AGP, Moreira JB, de Morais MG (2021) Microalgae polysaccharides: an overview of production, characterization, and potential applications. *Polysaccharides* 2:759–772. <https://doi.org/10.3390/polysaccharides2040046>
- Cruz D, Vasconcelos V, Pierre G, Michaud P, Delattre C (2020) Exopolysaccharides from cyanobacteria: strategies for bioprocess development. *Appl Sci* 10:3763. <https://doi.org/10.3390/app10113763>
- de Jesus Raposo MF, de Morais AMMB, de Morais RMSC (2014) Influence of sulphate on the composition and antibacterial and antiviral properties of the exopolysaccharide from *Porphyridium cruentum*. *Life Sci* 101:56–63. <https://doi.org/10.1016/j.lfs.2014.02.013>
- Delattre C, Pierre G, Laroche C, Michaud P (2016) Production, extraction and characterization of microalgal and cyanobacterial exopolysaccharides. *Biotechnol Adv* 34:1159–1179. <https://doi.org/10.1016/j.biotechadv.2016.08.001>
- Delran P, Frances C, Guihéneuf F, Peydecastaing J, Pontalier P-Y, Barthe L (2023) *Tetraselmis suecica* biofilm cell destruction by high-pressure homogenization for protein extraction. *Bioresour Technol Rep* 21:101372. <https://doi.org/10.1016/j.biteb.2023.101372>
- Destoumieux-Garzón D, Mavingui P, Boëtsch G, Boissier J, Darriet F, Duboz P, Fritsch C, Giraudoux P, Le Roux F, Morand S (2018) The one health concept: 10 years old and a long road ahead. *Front Vet Sci* 5:14. <https://doi.org/10.3389/fvets.2018.00014>
- Doghri I, Lavaud J, Dufour A, Bazire A, Lanneluc I, Sablé S (2017) Cell-bound exopolysaccharides from an axenic culture of the intertidal mudflat *Navicula phyllepta* diatom affect biofilm formation by benthic bacteria. *J Appl Phycol* 29:165–177. <https://doi.org/10.1007/s10811-016-0943-z>
- Dong B, Manolache S, Wong AC, Denes FS (2011) Antifouling ability of polyethylene glycol of different molecular weights grafted onto polyester surfaces by cold plasma. *Polym Bull* 66:517–528. <https://doi.org/10.1007/s00289-010-0358-y>
- Fanesi A, Paule A, Bernard O, Briandet R, Lopes F (2019) The architecture of monospecific microalgae biofilms. *Microorganisms* 7:352. <https://doi.org/10.3390/microorganisms7090352>
- Fanesi A, Martin T, Breton C, Bernard O, Briandet R, Lopes F (2022) The architecture and metabolic traits of monospecific photosynthetic biofilms studied in a custom flow-through system. *Biotechnol Bioeng* 119:2459–2470. <https://doi.org/10.1002/bit.28147>
- Fay F, Champion M, Guennec A, Moppert X, Simon-Colin C, Elie M (2023) Biobased anti-adhesive marine coatings from polyhydroxyalkanoates and polysaccharides. *Coatings* 13:766. <https://doi.org/10.3390/coatings13040766>
- Gadenne V, Lebrun L, Jouenne T, Thebault P (2015) Role of molecular properties of ulvans on their ability to elaborate antiadhesive surfaces. *J Biomed Mater Res, Part A* 103:1021–1028. <https://doi.org/10.1002/jbm.a.35245>
- Gargouch N, Elleuch F, Karkouch I, Tabbene O, Pichon C, Gardarin C, Rihouey C, Picton L, Abdelkafi S, Fendri I (2021) Potential of exopolysaccharide from *Porphyridium marinum* to contend with bacterial proliferation, biofilm formation, and breast cancer. *Mar Drugs* 19:66. <https://doi.org/10.3390/md19020066>
- Gomes L, Piard J-C, Briandet R, Mergulhão F (2017) *Pseudomonas grimontii* biofilm protects food contact surfaces from *Escherichia coli* colonization. *LWT-Food Sci Technol* 85:309–315. <https://doi.org/10.1016/j.lwt.2017.03.005>
- Guéneau V, Plateau-Gonthier J, Arnaud L, Piard J-C, Castex M, Briandet R (2022) Positive biofilms to guide surface microbial ecology in livestock buildings. *Biofilm* 4:100075. <https://doi.org/10.1016/j.biofilm.2022.100075>
- Guillard RR (1975) Culture of phytoplankton for feeding marine invertebrates. In: Smith ML, Chanley MH (eds) *Culture of Marine Invertebrates Animals*, Plenum Press, New York, p 29–60. https://doi.org/10.1007/978-1-4615-8714-9_3
- Guzmán F, Wong G, Román T, Cárdenas C, Álvarez C, Schmitt P, Albericio F, Rojas V (2019) Identification of antimicrobial peptides from the microalgae *Tetraselmis suecica* (Kyllin) Butcher and bactericidal activity improvement. *Mar Drugs* 17:453. <https://doi.org/10.3390/md17080453>
- Guzman-Murillo M, Ascencio F (2000) Anti-adhesive activity of sulphated exopolysaccharides of microalgae on attachment of red sore disease-associated bacteria and *Helicobacter pylori* to tissue culture cells. *Lett Appl Microbiol* 30:473–478. <https://doi.org/10.1046/j.1472-765x.2000.00751.x>
- Habimana O, Meyrand M, Meylheuc T, Kulakauskas S, Briandet R (2019) Genetic features of resident biofilms determine attachment of *Listeria monocytogenes*. *Appl Environ Microbiol* 75:7814–7821. <https://doi.org/10.1128/AEM.01333-09>
- Jiang P, Li J, Han F, Duan G, Lu X, Gu Y, Yu W (2011) Antibiofilm activity of an exopolysaccharide from marine bacterium *Vibrio sp* QY101. *PLoS One* 6:e18514. <https://doi.org/10.1371/journal.pone.0018514>
- Jun J-Y, Jung M-J, Jeong I-H, Yamazaki K, Kawai Y, Kim B-M (2018) Antimicrobial and antibiofilm activities of sulfated polysaccharides from marine algae against dental plaque bacteria. *Mar Drugs* 16:301. <https://doi.org/10.3390/md16090301>
- Junter G-A, Thebault P, Lebrun L (2016) Polysaccharide-based antibiofilm surfaces. *Acta Biomater* 30:13–25. <https://doi.org/10.1016/j.actbio.2015.11.010>
- Kermanshahi-Pour A, Sommer TJ, Anastas PT, Zimmerman JB (2014) Enzymatic and acid hydrolysis of *Tetraselmis suecica* for polysaccharide characterization. *Bioresour Technol* 173:415–421. <https://doi.org/10.1016/j.biortech.2014.09.048>
- Kim Y, Kim SH (2009) Released exopolysaccharide (r-EPS) produced from probiotic bacteria reduce biofilm formation of enterohemorrhagic *Escherichia coli* O157: H7. *Biochem Biophys Res Commun* 379:324–329. <https://doi.org/10.1016/j.bbrc.2008.12.053>
- Kives J, Orgaz B, SanJosé C (2006) Polysaccharide differences between planktonic and biofilm-associated EPS from *Pseudomonas fluorescens* B52. *Colloids Surf B* 52:123–27. <https://doi.org/10.1016/j.colsurfb.2006.04.018>
- Lauderdale KJ, Malone CL, Boles BR, Morcuende J, Horswill AR (2010) Biofilm dispersal of community-associated methicillin-resistant *Staphylococcus aureus* on orthopedic implant material. *J Orthop Res* 28:55–61
- Lauritano C, Andersen JH, Hansen E, Albrigtsen M, Escalera L, Esposito F, Helland K, Hanssen KØ, Romano G, Ianora A (2016) Bioactivity screening of microalgae for antioxidant, anti-inflammatory,

- anticancer, anti-diabetes, and antibacterial activities. *Front Mar Sci* 3:68. <https://doi.org/10.3389/fmars.2016.00068>
- Li SF, Fanesi A, Martin T, Lopes F (2023) Understanding *Chlorella vulgaris* acclimation strategies on textile supports can improve the operation of biofilm-based systems. *J Appl Phycol* 35:1061–1071. <https://doi.org/10.1007/s10811-023-02963-8>
- Loke MF, Lui SY, Ng BL, Gong M, Ho B (2007) Antiadhesive property of microalgal polysaccharide extract on the binding of *Helicobacter pylori* to gastric mucin. *FEMS Immunol Med Microbiol* 50:231–238. <https://doi.org/10.1111/j.1574-695X.2007.00248.x>
- Malone CL, Boles BR, Lauderdale KJ, Thoendel M, Kavanaugh JS, Horswill AR (2009) Fluorescent reporters for *Staphylococcus aureus*. *J Microbiol Methods* 77:251–260
- Mantzorou A, Ververidis F (2019) Microalgal biofilms: a further step over current microalgal cultivation techniques. *Sci Total Environ* 651:3187–3201. <https://doi.org/10.1016/j.scitotenv.2018.09.355>
- Marinho-Soriano E, Fonseca P, Carneiro M, Moreira W (2006) Seasonal variation in the chemical composition of two tropical seaweeds. *Bioresour Technol* 97:2402–2406. <https://doi.org/10.1016/j.biortech.2005.10.014>
- Mevo SIU, Ashrafudoulla M, Furkanur Rahaman Mizan M, Park SH, Ha SD (2021) Promising strategies to control persistent enemies: some new technologies to combat biofilm in the food industry—a review. *Compr Rev Food Sci Food Saf* 20:5938–5964. <https://doi.org/10.1111/1541-4337.12852>
- Murdock JN, Wetzel DL (2009) FT-IR microspectroscopy enhances biological and ecological analysis of algae. *Appl Spectrosc Rev* 44:335–361. <https://doi.org/10.1080/05704920902907440>
- Ofek I, Hasty DL, Sharon N (2003) Anti-adhesion therapy of bacterial diseases: prospects and problems. *FEMS Immunol Med Microbiol* 38:181–191. [https://doi.org/10.1016/S0928-8244\(03\)00228-1](https://doi.org/10.1016/S0928-8244(03)00228-1)
- Okana NA, Chalabaev S, Kim T-H, Fink A, Ross RA, Kasper DL (2013) Kdo hydrolase is required for *Francisella tularensis* virulence and evasion of TLR2-mediated innate immunity. *Mbio* 4:e00638-e712. <https://doi.org/10.1128/mBio.00638-12>
- Oniciuc E-A, Likotrafiti E, Alvarez-Molina A, Prieto M, López M, Alvarez-Ordóñez A (2019) Food processing as a risk factor for antimicrobial resistance spread along the food chain. *Curr Opin Food Sci* 30:21–26. <https://doi.org/10.1016/j.cofs.2018.09.002>
- Pandin C, Le Coq D, Canette A, Aymerich S, Briandet R (2017) Should the biofilm mode of life be taken into consideration for microbial biocontrol agents? *Microb Biotechnol* 10:719–734. <https://doi.org/10.1111/1751-7915.12693>
- Penaranda D, Bonnefond H, Guihéneuf F, Morales M, Bernard O (2023) Life cycle assessment of an innovative rotating biofilm technology for microalgae production: an eco-design approach. *J Cleaner Prod* 384:135600. <https://doi.org/10.1016/j.jclepro.2022.135600>
- Quémener B, Marot C, Mouillet L, Da Riz V, Diris J (2000) Quantitative analysis of hydrocolloids in food systems by methanolysis coupled to reverse HPLC. Part 1. Gelling Carrageenans *Food Hydrocoll* 14:9–17. [https://doi.org/10.1016/S0268-005X\(99\)00042-9](https://doi.org/10.1016/S0268-005X(99)00042-9)
- R Core Team (2013) R: a language and environment for statistical computing. R Foundation for Statistical Computing, Vienna, Austria. <http://www.R-project.org/>
- Rendueles O, Kaplan JB, Ghigo JM (2013) Antibiofilm polysaccharides. *Environ Microbiol* 15:334–346. <https://doi.org/10.1111/j.1462-2920.2012.02810.x>
- Risjani Y, Mutmainnah N, Manurung P, Wulan SN, Yunianta W (2021) Exopolysaccharide from *Porphyridium cruentum* (purpureum) is not toxic and stimulates immune response against vibriosis: the assessment using zebrafish and white shrimp *Litopenaeus vannamei*. *Mar Drugs* 19:133. <https://doi.org/10.3390/md19030133>
- Rizwan M, Mujtaba G, Memon SA, Lee K, Rashid N (2018) Exploring the potential of microalgae for new biotechnology applications and beyond: a review. *Renew Sustain Energy Rev* 92:394–404. <https://doi.org/10.1016/j.rser.2018.04.034>
- Ryther J, Guillard R (1962) Studies of marine planktonic diatoms: II. Use of *Cyclotella nana* Hustedt for assays of vitamin B12 in sea water. *Can J Microbiol* 8:437–445. <https://doi.org/10.1139/m62-057>
- Sansone C, Galasso C, Orefice I, Nuzzo G, Luongo E, Cutignano A, Romano G, Brunet C, Fontana A, Esposito F (2017) The green microalga *Tetraselmis suecica* reduces oxidative stress and induces repairing mechanisms in human cells. *Sci Rep* 7:41215. <https://doi.org/10.1038/srep41215>
- Scarsini M, Thurotte A, Veidl B, Amiard F, Niepceron F, Badawi M, Lagarde F, Schoefs B, Marchand J (2021) Metabolite quantification by Fourier transform infrared spectroscopy in diatoms: proof of concept on *Phaeodactylum tricornutum*. *Front Plant Sci* 12:756421. <https://doi.org/10.3389/fpls.2021.756421>
- Signorelli A, Aho K, Alfons A, Anderegg N, Aragon T, Arppe A, Baddeley A, Barton K, Bolker B, Borchers HW (2019) DescTools: tools for descriptive statistics. *R Packag Version* 0.99(28):17
- Soliemani O, Salimi F, Rezaei A (2022) Characterization of exopolysaccharide produced by probiotic *Enterococcus durans* DU1 and evaluation of its anti-biofilm activity. *Arch Microbiol* 204:419. <https://doi.org/10.1007/s00203-022-02965-z>
- Soto-Vásquez MR, Alvarado-García PAA, Youssef FS, Ashour ML, Bogari HA, Elhady SS (2022) FTIR characterization of sulfated polysaccharides obtained from *Macrocystis integrifolia* algae and verification of their antiangiogenic and immunomodulatory potency in vitro and in vivo. *Mar Drugs* 21:36. <https://doi.org/10.3390/md21010036>
- Srey S, Jahid IK, Ha S-D (2013) Biofilm formation in food industries: a food safety concern. *Food Control* 31:572–585. <https://doi.org/10.1016/j.foodcont.2012.12.001>
- Stead C, Tran A, Ferguson D Jr, McGrath S, Cotter R, Trent S (2005) A novel 3-deoxy-D-manno-octulosonic acid (Kdo) hydrolase that removes the outer Kdo sugar of *Helicobacter pylori* lipopolysaccharide. *J Bacteriol* 187:3374–3383. <https://doi.org/10.1128/JB.187.10.3374-3383.2005>
- Sun L, Wang C, Shi Q, Ma C (2009) Preparation of different molecular weight polysaccharides from *Porphyridium cruentum* and their antioxidant activities. *Int J Biol Macromol* 45:42–47. <https://doi.org/10.1016/j.ijbiomac.2009.03.013>
- Sun L, Wang L, Zhou Y (2012) Immunomodulation and antitumor activities of different-molecular-weight polysaccharides from *Porphyridium cruentum*. *Carbohydr Polym* 87:1206–1210. <https://doi.org/10.1016/j.carbpol.2011.08.097>
- Tabatabai M (1974) A rapid method for determination of sulfate in water samples. *Environ Lett* 7:237–243. <https://doi.org/10.1080/00139307409437403>
- Talyshinsky MM, Souprun YY, Huleihel MM (2002) Anti-viral activity of red microalgal polysaccharides against retroviruses. *Cancer Cell Int* 2:1–7. <https://doi.org/10.1186/1475-2867-2-8>
- Valle J, Da Re S, Henry N, Fontaine T, Balestrino D, Latour-Lambert P, Ghigo J-M (2006) Broad-spectrum biofilm inhibition by a secreted bacterial polysaccharide. *Proc Natl Acad Sci* 103:12558–12563. <https://doi.org/10.1073/pnas.0605399103>
- Vishwakarma J, Sirisha VL (2020) Unraveling the anti-biofilm potential of green algal sulfated polysaccharides against *Salmonella enterica* and *Vibrio harveyi*. *Appl Microbiol Biotechnol* 104:6299–314
- Vunduk J, Wan WAAQI, Mohamad SA, Abd Halim NH, Dzimir AZM, Žižak Ž, Klaus A (2019) Polysaccharides of *Pleurotus flabellatus* strain Mynuk produced by submerged fermentation as a promising novel tool against adhesion and biofilm formation of foodborne pathogens. *LWT* 112:108221. <https://doi.org/10.1016/j.lwt.2019.05.119>

- Wagner H, Jakob T, Fanesi A, Wilhelm C (2017) Towards an understanding of the molecular regulation of carbon allocation in diatoms: the interaction of energy and carbon allocation. *Philos Trans R Soc B* 372:20160410. <https://doi.org/10.1098/rstb.2016.0410>
- Wickham H (2016) *ggplot2: elegant graphics for data analysis*. Springer-Verlag, New York, USA, p 260
- Wittschier N, Lengsfeld C, Vortheims S, Stratmann U, Ernst J, Verspohl E, Hensel A (2007) Large molecules as anti-adhesive compounds against pathogens. *J Pharm Pharmacol* 59:777–786. <https://doi.org/10.1211/jpp.59.6.0004>
- Xiao R, Zheng Y (2016) Overview of microalgal extracellular polymeric substances (EPS) and their applications. *Biotechnol Adv* 34:1225–1244. <https://doi.org/10.1016/j.biotechadv.2016.08.004>
- Xu X, Peng Q, Zhang Y, Tian D, Zhang P, Huang Y, Ma L, Dia VP, Qiao Y, Shi B (2020) Antibacterial potential of a novel *Lactobacillus casei* strain isolated from Chinese northeast sauerkraut and the antibiofilm activity of its exopolysaccharides. *Food Funct* 11:4697–4706. <https://doi.org/10.1039/D0FO00905A>
- Zhang X, Wang L, Levänen E (2013) Superhydrophobic surfaces for the reduction of bacterial adhesion. *RSC Adv* 3:12003–12020. <https://doi.org/10.1039/C3RA40497H>
- Zheng S, Bawazir M, Dhall A, Kim H-E, He L, Heo J, Hwang G (2021) Implication of surface properties, bacterial motility, and hydrodynamic conditions on bacterial surface sensing and their initial adhesion. *Front Bioeng Biotechnol* 9:643722

Publisher's Note Springer Nature remains neutral with regard to jurisdictional claims in published maps and institutional affiliations.

Springer Nature or its licensor (e.g. a society or other partner) holds exclusive rights to this article under a publishing agreement with the author(s) or other rightsholder(s); author self-archiving of the accepted manuscript version of this article is solely governed by the terms of such publishing agreement and applicable law.